A Novel FFT-Based Robust Multivariable Process Identification Method

Qing-Guo Wang* and Yong Zhang

Department of Electrical Engineering, National University of Singapore, Singapore 119260, Singapore

In this paper, a general robust identification method is proposed for an interactive linear time-invariant multivariable process. Using the fast Fourier transform (FFT), the process frequency response matrix is first calculated from the recorded process input and output time responses. Then the process step response is constructed using the inverse FFT for each process channel. New linear regression equations are derived from such responses and their various-order integrals. The regression parameters are then estimated without iteration and give a first-order plus dead time model or a general second-order plus dead time model. The proposed method is applicable to various experimental scenarios. Its effectiveness is demonstrated through simulation examples and a real-time test.

1. Introduction

In process industries, most systems are multivariable in nature. The control of such multivariable processes has always been a challenge because of its complex interactive nature. Implementation of modern advanced controllers explicitly makes use of process models. Some of them such as model predictive control systems in the process industry are based upon nonparametric models,[1,2] while others such as internal model control require parametric models.[3−6] It is noted that most of the existing methods for parametric transfer function identification do not take into account the process delay (or dead time),[7] and delay is, however, present in most industrial processes and has significant implications on the achievable performance for control systems.

Process identification may also be classified into open-loop and closed-loop experiments. Performing identification experiments under a closed loop may be sometimes necessary because of safety or economic reasons or if the system contains inherent feedback mechanisms.[8] Comparatively, because of their simplicity and recent advance, open-loop experiments are still widely used and preferred in many applications. However, according to the authors' best knowledge, no method has been reported to cover both cases in a unified way.

Identification methods and results are influenced by identification tests devised. The typical test signals used in the process industry are step, relay, pseudo-random binary sequence, and sinusoidal functions.[9] Of all of these experiments, the step experiment is probably the simplest. The step experiment needs little equipment and can be performed easily. Therefore, the step experiment is still dominant in process control applications. There are many methods available for process identification from the step tests operated in open-loop[10−12] or closed-loop experiments.[13−16] However, most of them show no extension to multivariable processes. Recently, a new method to determine the open-loop process frequency response in a linear multivariable process based on a step change in the set point carried out during closed-loop proportional−integral−derivative (PID) control operation is presented by Melo and Friedly,[17] where no transfer function matrix for the process is given. For relay tests, Astrom and Hagglund[18] proposed a method to determine the approximate values of the ultimate gain and the ultimate frequency. Because the relay feedback identification has been proven to be very successful in industrial applications and has led to a number of commercial autotuners, its extension to a multivariable case has been in high demand and will continue to be appealing. Loh et al.[19] proposed a method which is a combination of sequential loop closing and relay tuning. Recently, a sequential relay feedback to identify the frequency response of a multivariable process was proposed by Wang et al.[1] using a fast Fourier transform (FFT)-based method. All of these methods give nonparametric models only. Compared with a step and/or relay experiment, an experiment with a multisine signal is time-consuming and is not easily implemented. Thus, even though many methods are available for this type of experiment,[20,21] they are not widely used in process control.

In view of the limitations of the existing multivariable identification methods, it is thus appealing that one general method be developed and applied to different scenarios in a unified way, covering both open-loop and closed-loop experiments, and all of the typical test signals with both nonparametric and parametric models available. Such a multivariable process identification method is presented in this paper. The recorded process inputs and outputs from tests are processed using the FFT to compute the frequency response matrix. The step response is further constructed using the inverse FFT (IFFT). New linear regression equations are derived from such a response and its various-order integrals. The regression parameters are then estimated with a least-squares method, and explicit relationships between the regression parameters and those in transfer functions are given. Because of the use of process output integrals in the regression equations, the resulting parameter estimation is very robust in the face of large measurement noise in the output.

The paper is organized as follows. In section 2, the proposed identification method is presented. In section 3, the method is illustrated through simulation ex-

* To whom all correspondence should be addressed. E-mail: elewqg@nus.edu.sg. Tel: (+65) 874 2282. Fax: (+65) 779 1103.

10.1021/ie9908175 CCC: $20.00
Published on Web 05/08/2001

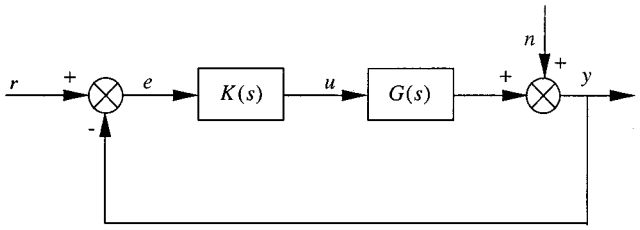

Figure 1. Multivariable feedback control system.

amples. A real-time experimental result is given in section 4. Conclusions are drawn in section 5.

2. Proposed Identification Method

In this paper, we assume that the process to be identified is linear time-invariant and that the test signals to be applied for identification purposes are persistently exciting, which roughly implies that all modes of the process are sufficiently excited during the identification experiment.[22] Consider the feedback system shown in Figure 1, where K is the controller and the $l \times m$ linear process is described by

$$\mathbf{Y}(s) = \mathbf{G}(s)\,\mathbf{U}(s) \tag{1}$$

with the output vector $\mathbf{Y}(s) = [Y_1(s)\ Y_2(s)\ \cdots\ Y_l(s)]^T$, the input vector $\mathbf{U}(s) = [U_1(s)\ U_2(s)\ \cdots\ U_m(s)]^T$, and the process transfer function matrix $\mathbf{G} = \{G_{ij}(s)\}$, with $i = 1, 2, ..., l$ and $j = 1, 2, ..., m$.

The idea of the proposed method is to calculate the process frequency response $\mathbf{G}(j\omega)$ using the FFT (subsection 2.1), construct for each entry the open-loop step response from $G_{ij}(j\omega)$ using the IFFT (subsection 2.2), and estimate a transfer function from such a response (subsection 2.3).

For simplicity of exposition, our method is illustrated for the case of the closed-loop sequential relay experiment, as depicted in Figure 2. The closed-loop sequential relay experiment on an $l \times m$ process is actually executed as follows:

Initialization. Bring the process to constant steady states $y(0)$ and $u(0)$ at $t_0 = 0$. Specify the ith relay amplitude β_i, with $i = 1, 2, ..., m$.

Test 1. Apply the first relay test to the first input r_1, while keeping all other inputs r_i unchanged. Wait for the system to settle down at $t = t_1$; that is, the output y has reached stationary oscillations.

Test i. Apply the ith relay test to the ith input r_i at $t = t_{i-1}$, with $i = 2, 3, ..., m$, while the previous changes are still in place. Wait until the system settles down again at $t = t_i$.

The process output and input responses from all of these m tests are collected and denoted by $\{u(t), y(t), t \in [t_0, t_m]\}$.

2.1. Process Frequency Response. It can be seen from (1) that if one has m independent output and input frequency response vectors $\tilde{Y}^i(j\omega)$ and $\tilde{U}^i(j\omega)$, the process frequency response matrix $\mathbf{G}(j\omega)$ can then be obtained from the equation

$$[\tilde{Y}^1(j\omega)\ \tilde{Y}^2(j\omega)\ \cdots\ \tilde{Y}^m(j\omega)] = \mathbf{G}(j\omega)\,[\tilde{U}^1(j\omega)\ \tilde{U}^2(j\omega)\ \cdots\ \tilde{U}^m(j\omega)]$$

Our task now is to construct m independent time response vectors $\tilde{y}^i(t)$ and $\tilde{u}^i(t)$ from the recorded process output and input responses $y(t)$ and $u(t)$ such that, for each i, $\tilde{y}^i(t)$ and $\tilde{u}^i(t)$ have zero initial conditions at start and steady states in the end and their frequency responses $\tilde{Y}^i(j\omega)$ and $\tilde{U}^i(j\omega)$ meet $\tilde{Y}^i(j\omega) = \mathbf{G}(j\omega)\,\tilde{U}^i(j\omega)$. For the closed-loop relay experiment which leads to stationary oscillations, making $\tilde{y}(t_{i-1}) = 0$ only is not enough because its derivations could still be nonzero. Instead, let us imagine that, for each i, the ith test lasts beyond $t = t_i$ until $t = t_m$ without activating the subsequent tests; then the last cycle of stationary oscillations $y_s^i(t)$ and $u_s^i(t)$ sustained before $t = t_i$ will be repeated until $t = t_m$. One can thus define for each i

$$\tilde{y}^i(t) = \begin{cases} y(t) - y(0), & 0 \leq t < t_i \\ y_s^i(t) - y(0), & t_i \leq t \leq t_m \end{cases} \tag{2a}$$

and

$$\tilde{u}_i(t) = \begin{cases} u(t) - u(0), & 0 \leq t < t_i \\ u_s^i(t) - u(0), & t_i \leq t \leq t_m \end{cases} \tag{2b}$$

$\tilde{y}^i(t)$ and $\tilde{u}^i(t)$ have transients and do not decay to zero. They are thus neither absolutely integrable nor periodic and cannot be treated directly using Fourier transform to get the process frequency response $\mathbf{G}(j\omega)$.[23] Decom-

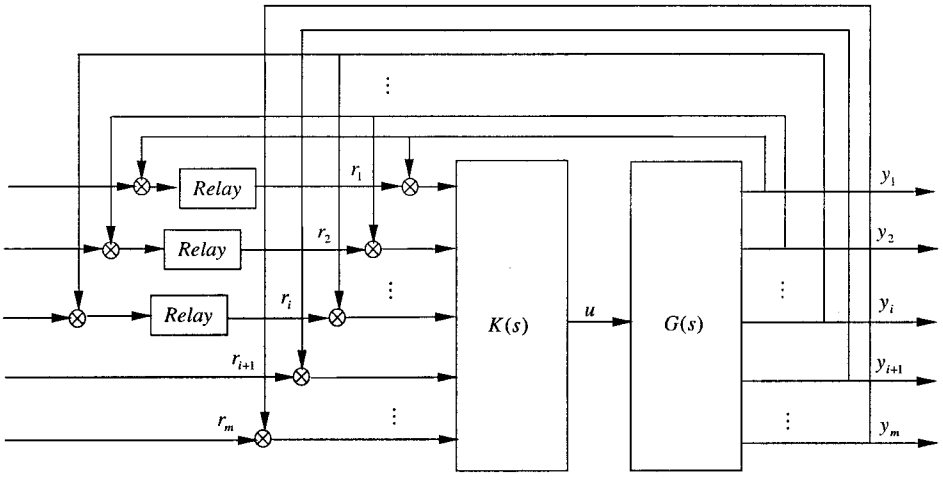

Figure 2. Closed-loop sequential relay feedback experiment.

pose the responses into the transient parts and steady-state parts as

$$\tilde{y}^i(t) = \Delta\tilde{y}^i(t) + \tilde{y}^i_s(t), \quad i = 1, 2, ..., m \tag{3a}$$

$$\tilde{u}^i(t) = \Delta\tilde{u}^i(t) + \tilde{u}^i_s(t), \quad i = 1, 2, ..., m \tag{3b}$$

Under each test i, $\tilde{y}^i(t)$ and $\tilde{u}^i(t)$ have almost entered the steady states at $t = t_i$, and both $\Delta\tilde{y}^i(t)$ and $\Delta\tilde{u}^i(t)$ are approximately zero afterward. The Fourier transform of $\Delta\tilde{y}^i(t)$ then gives its frequency response

$$\Delta\tilde{Y}^i(j\omega) = \int_0^\infty \Delta\tilde{y}^i(t)\, e^{-j\omega t}\, dt \tag{4}$$

In practice, (4) is approximated by

$$\Delta\tilde{Y}^i(j\omega) \approx \int_0^{t_m} \Delta\tilde{y}^i(t)\, e^{-j\omega t}\, dt \tag{5}$$

(5) can be computed at discrete frequencies using the standard FFT technique, which is a fast algorithm for calculating the discrete Fourier transform (DFT). The FFT of one period/several periods of the periodic part or the constant steady-state part $\tilde{y}^i_s(t)$ ($\tilde{u}^i_s(t)$) will actually give the scaled *coefficients* of the corresponding *Fourier series* of $\tilde{y}^i_s(t)$ ($\tilde{u}^i_s(t)$) or the scaled *amplitudes* of the impulses of the *extended Fourier transform* of $\tilde{y}^i_s(t)$ ($\tilde{u}^i_s(t)$).[24,25] The FFT results of the transient parts and the steady-state parts thus have different meanings, and they cannot be added together. We have to treat $\tilde{y}^i_s(t)$ and $\tilde{u}^i_s(t)$ specially to find their frequency responses $\tilde{Y}^i_s(j\omega)$ and $\tilde{U}^i_s(j\omega)$.

For the relay experiment causing stationary oscillations, it then follows from Kuhfitting[26] that

$$\tilde{Y}^i_s(j\omega) = \frac{1}{1 - e^{-j\omega T_i}} \int_{t_i - T_i}^{t_i} \tilde{y}^i_s(t)\, e^{-j\omega(t + T_i - t_i)}\, dt \tag{6}$$

where T_i is the period of the stationary oscillations of $\tilde{y}^i_s$. Similarly, the following expression can be obtained:

$$\tilde{U}^i_s(j\omega) = \frac{1}{1 - e^{-j\omega T_i}} \int_{t_i - T_i}^{t_i} \tilde{u}^i_s(t)\, e^{-j\omega(t + T_i - t_i)}\, dt \tag{7}$$

For each test i, it follows from (1) that there holds the frequency response relation

$$\tilde{Y}^i(j\omega) = G(j\omega)\, \tilde{U}^i(j\omega), \quad i = 1, 2, ..., m \tag{8}$$

where

$$\tilde{Y}^i(j\omega) = \Delta\tilde{Y}^i(j\omega) + \tilde{Y}^i_s(j\omega) \tag{9a}$$

$$\tilde{U}^i(j\omega) = \Delta\tilde{U}^i(j\omega) + \tilde{U}^i_s(j\omega) \tag{9b}$$

are obtained from (4)−(7). Collecting (8) for all i gives

$$\bar{Y}(j\omega) = G(j\omega)\, \bar{U}(j\omega) \tag{10}$$

where

$$\bar{Y}(j\omega) = [\tilde{Y}^1(j\omega)\ \tilde{Y}^2(j\omega) \cdots \tilde{Y}^m(j\omega)]$$

$$\bar{U}(j\omega) = [\tilde{U}^1(j\omega)\ \tilde{U}^2(j\omega) \cdots \tilde{U}^m(j\omega)]$$

It follows from Figure 1 that

$$U(s) = K(s)\,[I + G(s)\,K(s)]^{-1} R(s) \triangleq Q(s)\,R(s) \tag{11}$$

with nonsingular $Q(s)$, or in a frequency domain

$$\bar{U}(j\omega) = Q(j\omega)\, \bar{R}(j\omega) \tag{12}$$

Because $\bar{R}(j\omega)$ resulting from a sequential test has an upper triangular form and is nonsingular, it then follows from (12) that $\bar{U}(j\omega)$ is also nonsingular for $\omega \in [0, \infty)$.

Therefore, the process frequency response is obtained from (10) as

$$G(j\omega) = [\Delta\tilde{Y}^1(j\omega) + \tilde{Y}^1_s(j\omega) \cdots \Delta\tilde{Y}^m(j\omega) + \tilde{Y}^m_s(j\omega)][\Delta\tilde{U}^1(j\omega) + \tilde{U}^1_s(j\omega) \cdots \Delta\tilde{U}^m(j\omega) + \tilde{U}^m_s(j\omega)]^{-1} \tag{13}$$

which is valid at all $\omega \in [0, \infty)$.

Remark 1. To implement this procedure in real time, one must specify values for the time span T^i_f, $i = 1, 2, ..., m$ of the ith relay test. Following the discussion in Wang et al.,[27] T^i_f is given by $T^i_f = (N - 1)T_s$ with $N \approx (M - 1)T_i/T_s$, where T_s is the sampling time, and M should be specified a priori and should be large enough to ensure that the stationary oscillations are reached.

Remark 2. In practice, measurements are more or less sensitive to noise. It is apparent that a large signal-to-noise ratio is desirable.[10] Further, noise reduction techniques such as hysteresis, filter, and averaging strategy[27] can be adopted to produce a better estimation of the process frequency response matrix.

2.2. Construction of Process Step Response. Given the frequency response matrix $G(j\omega)$, the step response of each entry can be constructed separately. Because this construction involves only a single-input and single-output problem in an elementwise way, for simplicity of presentation we will, in this and the next subsections, drop subscripts i and j in G_{ij} and simply use $Y(s) = G(s)\,U(s)$ to denote scalar output $Y(s)$, scalar input $U(s)$, and scalar transfer function $G(s)$.

Imagine that the input $u(t)$ to G is the unit step, then the output Laplace transform is

$$Y(s) = G(s)\,\frac{1}{s} \tag{14}$$

It seems very easy to obtain the time response $y(t)$ by simply applying the inverse Fourier transform to $Y(j\omega)$. However, because the steady-state part of $y(t)$ is nonzero, $y(t)$ is not absolutely integrable and thus not Fourier transformable.[25] To solve this obstacle, $y(t)$ is decomposed into

$$y(t) = y(\infty) + \Delta y(t) = G(0) + \Delta y(t) \tag{15}$$

Applying the Laplace transform to both sides gives

$$Y(s) = \frac{G(0)}{s} + \mathcal{L}\{\Delta y(t)\} \tag{16}$$

Bringing (14) in, we have

$$\mathcal{L}\{\Delta y(t)\} = \frac{G(s) - G(0)}{s}$$

Note that $\Delta y(t)$ is the transient response and decays to zero for a stable system, and thus it is Fourier transformable.[25] One then has

$$\Delta y(t) = F^{-1}\left\{\frac{G(j\omega) - G(0)}{j\omega}\right\}$$

where F^{-1} is the inverse Fourier transform and can be implemented effectively and efficiently by the IFFT algorithm. Therefore, it follows from (15) that the output step response is constructed from its frequency response as

$$y(t) = G(0) + F^{-1}\left\{\frac{G(j\omega) - G(0)}{j\omega}\right\} \tag{17}$$

2.3. Process Transfer Function. We are now ready to estimate a model $\hat{G}(s)$ from the constructed step response $y(t)$. The process model is supposed to be a first-order plus dead-time (FOPDT) or second-order plus dead-time (SOPDT), which is adequate to describe most industrial processes.[28,29] The model is written as

$$Y(s) = \hat{G}(s)\,U(s) = \frac{b_{n-1}s^{n-1} + \ldots + b_1 s + 1}{a_n s^n + \ldots + a_1 s + a_0} e^{-Ls} U(s), \quad n = 1 \text{ or } 2 \tag{18}$$

where $a_0 = 1/G(0)$ is readily available. For $n = 1$, a FOPDT model is obtained which describes a linear monotonic process quite well in most chemical processes. However, for plants such as mechanical systems whose behavior is very different from FOPDT processes, a SOPDT model, i.e., $n = 2$ in (18), should be used. Such a SOPDT model can describe some nonminimum-phase processes with one dominant right-half-plane zero as well as second-order minimum-phase processes.

(18) is written equivalently in the time domain

$$a_n y^{(n)}(t) + \ldots + a_1 \dot{y}(t) + a_0 y(t) = b_{n-1} u^{(n-1)}(t - L) + \ldots + b_1 \dot{u}(t - L) + u(t - L) \tag{19}$$

For an integer $m \geqslant 1$, we define

$$\int_{[0,t]}^{(m)} f(t) = \underbrace{\int_0^t \int_0^{\tau_m} \cdots \int_0^{\tau_2}}_{m} f(\tau_1)\, d\tau_1 \cdots d\tau_m$$

Under zero initial condition, integrating (19) n times yields

$$a_n y(t) + a_{n-1}\int_{[0,t]}^{(1)} y(t) + \ldots + a_0 \int_{[0,t]}^{(n)} y(t) = b_{n-1}\int_{[0,t]}^{(1)} u(t - L) + \ldots + b_1 \int_{[0,t]}^{(n-1)} u(t - L) + \int_{[0,t]}^{(n)} u(t - L) \tag{20}$$

For the assumed unit step input $u(t) = \mathbf{1}(t)$, there holds

$$\int_{[0,t]}^{(m)} u(t - L) = \frac{1}{m!}(t - L)^m, \quad t \geqslant L \tag{21}$$

For $t \geqslant L$, substituting (21) into (20) gives

$$-a_0 \int_{[0,t]}^{(n)} y(t) = a_n y(t) + a_{n-1}\int_{[0,t]}^{(1)} y(t) + \ldots + a_1 \int_{[0,t]}^{(n-1)} y(t) - b_{n-1}(t - L) - \ldots - \frac{1}{(n-1)!} b_1 (t - L)^{n-1} - \frac{1}{n!}(t - L)^n \tag{22}$$

For $n = 1$, (22) becomes

$$t - a_0 \int_0^t y(\tau)\, d\tau = a_1 y(t) + L \tag{23}$$

Define

$$\begin{cases} \gamma(t) = t - a_0 \int_0^t y(t)\, d\tau \\ \phi(t) = [y(t) \quad 1]^T \\ \boldsymbol{\theta} = [a_1 \quad L]^T \end{cases} \tag{24}$$

(23) can be expressed as

$$\gamma(t) = \phi^T \boldsymbol{\theta}(t) \tag{25}$$

Invoke (25) for $t = t_i$, $i = 1, 2, \ldots, N$, $L \leqslant t_1 < t_2 < \ldots < t_N$, to form the regression form

$$\boldsymbol{\Gamma} = \boldsymbol{\Phi}\boldsymbol{\theta} \tag{26}$$

where $\boldsymbol{\Gamma} = [\gamma(t_1), \gamma(t_2), \ldots, \gamma(t_N)]^T$ and $\boldsymbol{\Phi} = [\phi(t_1), \phi(t_2), \ldots, \phi(t_N)]^T$. The ordinary LS can be applied to (26) to find its solution:

$$\hat{\theta} = (\boldsymbol{\Phi}^T\boldsymbol{\Phi})^{-1}\boldsymbol{\Phi}^T\boldsymbol{\Gamma} \tag{27}$$

In real applications, the actual measurement of the process outputs under the identification experiment is inevitably corrupted by measurement noise, which leads to the corruption of the constructed $y(t)$. In such a case, the IV method can be applied to give a consistent estimate.[22] For our case, the instrumental variable matrix $\mathbf{Z}$ is chosen as

$$\mathbf{Z} = \begin{bmatrix} \frac{1}{t_1} & t_1^2 \\ \vdots & \vdots \\ \frac{1}{t_N} & t_N^2 \end{bmatrix} \tag{28}$$

and the estimate is thus given by

$$\hat{\theta} = (\mathbf{Z}^T\boldsymbol{\Phi})^{-1}\mathbf{Z}^T\boldsymbol{\Gamma} \tag{29}$$

Once $\hat{\theta}$ is found from (27), one can recover a_1 and L:

$$\begin{bmatrix} a_1 \\ L \end{bmatrix} = \begin{bmatrix} \hat{\theta}_1 \\ \hat{\theta}_2 \end{bmatrix} \tag{30}$$

Similarly, for $n = 2$, (22) becomes

$$-a_0 \int_0^t \int_0^\tau y(\tau_1)\, d\tau_1\, d\tau = a_2 y(t) + a_1 \int_0^t y(\tau)\, d\tau - b_1(t - L) - \frac{1}{2}(t - L)^2 \tag{31}$$

Rearrange (31) to get

$$\frac{1}{2}t^2 - a_0 \int_0^t \int_0^\tau y(\tau_1)\, d\tau_1\, d\tau = a_2 y(t) + a_1 \int_0^t y(\tau)\, d\tau + (L - b_1)t + b_1 L - \frac{1}{2}L^2 \tag{32}$$

It is again expressed as

$$\gamma(t) = \phi^T \boldsymbol{\theta}(t) \tag{33}$$

where

$$\begin{cases} \gamma(t) = \frac{1}{2}t^2 - a_0 \int_0^t \int_0^t y(\tau_1)\, d\tau_1\, d\tau \\ \phi(t)^T = [y(t) \quad \int_0^t y(t)\, d\tau \quad t \quad 1]^T \\ \boldsymbol{\theta} = \left[a_2 \quad a_1 \quad L - b_1 \quad b_1 L - \frac{1}{2}L^2\right]^T \end{cases} \tag{34}$$

Invoke (33) for $t = t_i \geq L$, $i = 1, 2, ..., N$, to form the regression form

$$\boldsymbol{\Gamma} = \boldsymbol{\Phi}\boldsymbol{\theta} \tag{35}$$

where $\boldsymbol{\Gamma} = [\gamma(t_1), \gamma(t_2), ..., \gamma(t_N)]^T$ and $\boldsymbol{\Phi} = [\phi(t_1), \phi(t_2), ..., \phi(t_N)]^T$. The ordinary LS technique can be applied directly to find its solution as stated in (27). In the case of measurement noise, the IV method is applied to find the solution as (29), where $\mathbf{Z}$ is set as

$$\mathbf{Z} = \begin{bmatrix} \frac{1}{t_1^2} & \frac{1}{t_1} & t_1^2 & t_1^3 \\ \vdots & \vdots & \vdots & \vdots \\ \frac{1}{t_N^2} & \frac{1}{t_N} & t_N^2 & t_N^3 \end{bmatrix}$$

The process parameters, a_2, a_1, b_1, and L, can be recovered as

$$\begin{bmatrix} a_2 \\ a_1 \\ b_1 \\ L \end{bmatrix} = \begin{bmatrix} \hat{\theta}_1 \\ \hat{\theta}_2 \\ \pm\sqrt{\hat{\theta}_3^2 + 2\hat{\theta}_4} \\ \hat{\theta}_3 + b_1 \end{bmatrix} \tag{36}$$

A negative b_1 corresponds to a nonminimum-phase process and will cause inverse response; i.e., the response will first move in a direction opposite to its final value. A positive b_1 corresponds to a minimum-phase process. Thus, by observing the output time response, one is able to determine b_1 by

$$b_1 = \begin{cases} -\sqrt{\hat{\theta}_3^2 + 2\hat{\theta}_4}, & \text{if an inverse response is detected} \\ \sqrt{\hat{\theta}_3^2 + 2\hat{\theta}_4}, & \text{otherwise} \end{cases}$$

This rule always works well if the underlining process is of second-order or of a second-order-dominated one.

Remark 3. In practice, the selection of $t_i \geq L$ can be made as follows:

$$\text{abs}\{\text{mean}[y(t_i - \tau, t_i)]\} > 2B_n$$

where B_n is the noise band and τ is the user-specified time interval used for averaging. After extensive simulation, the default value of t_N is set as $1.5T_{set}$, where T_{set} is the settling time, defined as the time required for the process to settle within ±2% of its steady state. For the case with a large number of $y(t_i)$ values available, the default value of N is recommended as 200, and t_i may be set as

$$t_i = t_1 + \frac{i-1}{N}(t_N - t_1), \quad i = 1, 2, ..., N$$

2.4. Identification Algorithm. The proposed identification algorithm is summarized as follows:

Initialization: Bring the process to the constant steady states.

Step 1: Perform the closed-loop sequential relay experiment and record all of the process input and process output responses.

Step 2: Calculate the frequency response $G(j\omega)$ from (13).

Step 3: Construct the process step response from (17).

Step 4: Estimate the FOPDT models in (18) from (27) or (29) and (30) or the SOPDT models in (18) from (27) or (39) and (36).

Remark 4. For illustration, the closed-loop sequential relay experiment has been considered so far. However, it should be pointed out that the identification scheme proposed above can be easily extended with trivial modifications to other types of experiments, covering various test signals, closed-loop/open-loop, and sequential and decentralized experiments with any type of controller, provided that the process is linear time invariant, the system under experiment is stable, and each test generates a steady state. For an experiment such as step tests, which gives constant steady states, different from (2), to have signals with zero conditions, one only needs to subtract the output and input by their initial conditions and thus form the modified signals as

$$\tilde{y}^i(t) = y(t) - y(t_{i-1}), \qquad t_{i-1} \leq t < t_i, \quad i = 1, 2, ..., m$$

$$\tilde{u}^i(t) = u(t) - u(t_{i-1}), \qquad t_{i-1} \leq t < t_i, \quad i = 1, 2, ..., m$$

Another difference for a step experiment from a relay experiment lies in $\tilde{Y}_s^i(j\omega) = \tilde{y}_s^i(t_i)/j\omega$, with $i = 1, 2, ..., m$, instead of the one in (6). Once the process frequency response matrix is calculated, the remaining two steps for the process step response and the transfer function model calculations are the same as those described in subsections 2.2 and 2.3. The details for various experiments are documented in Wang and Zhang.[30]

Remark 5. The proposed method can give nonparametric models as well as parametric models. For the parametric model estimation, the process step response is constructed first. The FFT and IFFT are inexpensive computations, and only linear least squares or an instrumental variable method is involved in FOPDT/SOPDT modeling from step responses. Moreover, the method can be easily extended to obtain higher-order transfer functions as discussed in Wang and Zhang.[31]

Remark 6. The combined use of the FFT and IFFT is crucial for enhancement of the identification performance. It looks possible and reasonable to estimate the process frequency response with the FFT and then obtain a transfer function to match the frequency response directly. However, simple experiments such as step or relay cannot excite the process effectively and uniformly over the whole working frequency range, and the error of the frequency response estimation varies with frequencies. This may in turn cause poor identification of the transfer function matrix. We find that the error inherent in the process frequency response with the FFT is neutralized or compensated for by the later IFFT so that the process step response can be recovered accurately and leads to better transfer functions, which will be demonstrated in our simulation in section 3.

3. Simulation Examples

In this section, the proposed identification method is applied to two industrial processes to show the ef-

fectiveness. For a better assessment of its accuracy, identification errors in both the time and frequency domains are considered. To achieve a better control performance, the estimation error should be small in both the time and frequency domains. The time domain identification error is measured over the transient period by the relative standard deviation:[32]

$$\epsilon_i = \frac{\sum_{k=1}^{N}[y_i(kT_s) - \hat{y}_i(kT_s)]^2}{\sum_{k=1}^{N} y_i^2(kT_s)} \times 100\% \qquad (37)$$

where $y_i(kT_s)$, with $i = 1, 2, ..., l$, are the actual outputs under the identification experimental experiment, while $\hat{y}_i(kT_s)$, with $i = 1, 2, ..., l$, are the responses of the estimated transfer function under the recorded same inputs and are generated by simulation. The frequency domain identification error is measured by the *worst-case relative error*:

$$E = \max_k \left\{ \left| \frac{\hat{G}_{ij}(j\omega_k) - G_{ij}(j\omega_k)}{G_{ij}(j\omega_k)} \right| \times 100\%,\ k = 1, 2, ..., M \right\} \qquad (38)$$

where $G_{ij}(j\omega_i)$ and $\hat{G}_{ij}(j\omega_i)$, with $i, j = 1, 2, ..., m$, are the actual and the estimated process frequency responses, respectively. The Nyquist curve for a phase ranging from 0 to $-\pi$ is considered, because this part is the most significant for control design.

In practice, the measurement noise is generally present. In the context of system identification, the noise-to-signal ratio[33] is usually defined as

$$\mathrm{NSR} = \frac{\mathrm{mean[abs(noise)]}}{\mathrm{means[abs(signal)]}}$$

Example 1. Consider the well-known Wood−Berry (WB) binary distillation column plant:[34]

$$\mathbf{G}(s) = \begin{bmatrix} \frac{12.8e^{-s}}{16.7s+1} & \frac{-18.9e^{-3s}}{21s+1} \\ \frac{6.6e^{-7s}}{10.9s+1} & \frac{-19.4e^{-3s}}{14.4s+1} \end{bmatrix}$$

Suppose that the process is under the control of a decentralized PI controller:[4]

$$\mathbf{K}(s) = \begin{bmatrix} 0.38 + \frac{0.045}{s} & 0 \\ 0 & -0.075 - \frac{0.0032}{s} \end{bmatrix}$$

and the process is at a constant steady state. With the controller in action, a closed-loop sequential relay feedback experiment is carried out on top of it. A relay with the amplitude of 1 and the bias of 0.1 is first applied to the first loop while the second loop is kept unattached. When stationary oscillations are reached at $t = 200$, a relay test is made in the second loop with the amplitude of 1 and the bias of 0.1 until $t = 400$, while the previous change in the first loop is still in place. Then the proposed method gives the estimated model

$$\hat{G}(s) = \begin{bmatrix} \frac{12.8000e^{-1.0009s}}{16.7050s+1} & \frac{-18.9000e^{-3.0009s}}{21.0050s+1} \\ \frac{6.6000e^{-7.0009s}}{10.9050s+1} & \frac{-19.4000e^{-3.0009s}}{14.4050s+1} \end{bmatrix}$$

where the errors are

$$\epsilon = \begin{bmatrix} 0.006227\% \\ 0.01352\% \end{bmatrix}$$

and

$$E = \begin{bmatrix} 0.1458\% & 0.0562\% \\ 0.0563\% & 0.0639\% \end{bmatrix}$$

respectively.

Suppose now that some fast dynamics are taken into consideration to get

$$\mathbf{G}(s) = \begin{bmatrix} \frac{12.8e^{-s}}{16.7s+1} & \frac{-18.9e^{-3s}}{(21s+1)(0.5s+1)^3} \\ \frac{6.6e^{-7s}}{10.9s+1} & \frac{-19.4e^{-3s}}{(14.4s+1)(2s+1)^3} \end{bmatrix}$$

The identified FOPDT model is

$$\hat{G}(s) = \begin{bmatrix} \frac{12.8000e^{-1.0012s}}{16.7100s+1} & \frac{-18.9000e^{-4.5010s}}{21.0084s+1} \\ \frac{6.6000e^{-7.0011s}}{10.9053s+1} & \frac{-19.400e^{-8.5038s}}{17.2503s+1} \end{bmatrix}$$

with

$$\epsilon = \begin{bmatrix} 0.2883\% \\ 0.037272\% \end{bmatrix}$$

and

$$E = \begin{bmatrix} 0.1461\% & 3.4834\% \\ 0.0564\% & 10.0421\% \end{bmatrix}$$

respectively. As expected, a larger error in $\hat{G}_{22}(s)$ than that in $\hat{G}_{12}(s)$ exists where the impact of the fast dynamics is more severe. To improve the accuracy, second-order models for $G_{12}(s)$ and $G_{22}(s)$ are identified to yield

$$\hat{G}(s) = \begin{bmatrix} \frac{12.8000e^{-1.0012s}}{16.7100s+1} & \frac{-18.9000e^{-3.7772s}}{15.2929s^2+21.7327s+1} \\ \frac{6.6000e^{-7.0011s}}{10.9053s+1} & \frac{-19.400e^{-5.6027s}}{50.2513s^2+17.7990s+1} \end{bmatrix}$$

with

$$\epsilon = \begin{bmatrix} 0.09282\% \\ 0.02502\% \end{bmatrix}$$

and

$$E = \begin{bmatrix} 0.1461\% & 2.7190\% \\ 0.0564\% & 3.5746\% \end{bmatrix}$$

respectively. It is also possible to produce third-order

Table 1. Identification Results for the WB Plant under Different NSRs

	proposed			
NSR	$\hat{G}(s)$	ϵ	E	E (Melo's)
0	$\begin{bmatrix} \frac{12.80e^{-1.00s}}{16.71s+1} & \frac{-18.90e^{-3.00s}}{21.01s+1} \\ \frac{6.60e^{-7.00s}}{10.91s+1} & \frac{-19.40e^{-3.00s}}{14.41s+1} \end{bmatrix}$	$\begin{bmatrix} 0.06227\% \\ 0.01352\% \end{bmatrix}$	$\begin{bmatrix} 0.15\% & 0.06\% \\ 0.06\% & 0.06\% \end{bmatrix}$	$\begin{bmatrix} 0.72\% & 0.27\% \\ 0.29\% & 0.33\% \end{bmatrix}$
5%	$\begin{bmatrix} \frac{12.74e^{-0.98s}}{16.72s+1} & \frac{-19.07e^{-2.96s}}{21.16s+1} \\ \frac{6.50e^{-7.00s}}{10.80s+1} & \frac{-19.51e^{-2.92s}}{14.62s+1} \end{bmatrix}$	$\begin{bmatrix} 2.80\% \\ 5.50\% \end{bmatrix}$	$\begin{bmatrix} 3.52\% & 2.25\% \\ 1.52\% & 4.08\% \end{bmatrix}$	$\begin{bmatrix} 88.08\% & 16.06\% \\ 5.07\% & 23.89\% \end{bmatrix}$
10%	$\begin{bmatrix} \frac{12.67e^{-0.95s}}{16.73s+1} & \frac{-9.25e^{-2.91s}}{21.31s+1} \\ \frac{6.39e^{-7.04s}}{10.87s+1} & \frac{-19.62e^{-2.81s}}{14.89s+1} \end{bmatrix}$	$\begin{bmatrix} 5.72\% \\ 17.21\% \end{bmatrix}$	$\begin{bmatrix} 7.10\% & 4.61\% \\ 3.14\% & 10.25\% \end{bmatrix}$	$\begin{bmatrix} 173.65\% & 32.56 \\ 9.49\% & 50.54\% \end{bmatrix}$
20%	$\begin{bmatrix} \frac{12.52e^{-0.93s}}{16.75s+1} & \frac{-19.60e^{-2.87s}}{21.48s+1} \\ \frac{6.16e^{-7.00s}}{10.86s+1} & \frac{-19.85e^{-2.70s}}{15.18s+1} \end{bmatrix}$	$\begin{bmatrix} 18.44\% \\ 35.83\% \end{bmatrix}$	$\begin{bmatrix} 11.12\% & 7.22\% \\ 6.73\% & 16.11\% \end{bmatrix}$	$\begin{bmatrix} 334.08\% & 61.27\% \\ 17.71\% & 111.58\% \end{bmatrix}$
30%	$\begin{bmatrix} \frac{12.34e^{-0.86s}}{16.80s+1} & \frac{-19.95e^{-2.71s}}{22.01s+1} \\ \frac{5.88e^{-7.01s}}{10.81s+1} & \frac{-20.07e^{-2.33s}}{16.12s+1} \end{bmatrix}$	$\begin{bmatrix} 38.67\% \\ 47.51\% \end{bmatrix}$	$\begin{bmatrix} 22.36\% & 15.12\% \\ 10.90\% & 35.02\% \end{bmatrix}$	$\begin{bmatrix} 411.14\% & 80.04\% \\ 26.70\% & 184.80\% \end{bmatrix}$

models for $G_{12}(s)$ and $G_{22}(s)$ to get

$$\hat{G}(s) = \begin{bmatrix} \frac{12.8000e^{-1.0012s}}{16.7100s+1} & -\frac{-2.2690s^2+101.6138s+18.9000}{68.9655s^3+129.4690s^2+27.0897s+1}e^{-3.8684s} \\ \frac{6.6000e^{-7.0011s}}{10.9053s+1} & -\frac{21.7813s^2+12.8672s+19.4}{78.1250s^2+71.6719s^2+19.039s+1}e^{-5.0823s} \end{bmatrix}$$

with even smaller errors

$$\epsilon = \begin{bmatrix} 0.07213\% \\ 0.01855\% \end{bmatrix}$$

and

$$E = \begin{bmatrix} 0.1461\% & 1.6266\% \\ 0.0564\% & 0.2912\% \end{bmatrix}$$

respectively. It is, however, noticed that SOPDT models have achieved good accuracy.

Because the proposed method makes use of many points rather than one or two points on the process response and adopts a LS or an IV method, it is expected to be robust to measurement noise n shown in Figure 1. To demonstrate this, the WB process is again tested under different noise levels. For comparison, Melo's method[17] for the estimation of the process frequency response is also tested under the same conditions. The results are listed in Table 1. The robustness of the proposed method is evident. Figures 3 and 4 show the Bode plots for G_{11} and G_{22} of this WB plant under NSR = 30%, respectively, where the dashed line is for the actual plant, the solid line for the model from our method, × for the proposed FFT algorithm without further IFFT and transfer function modeling, and ○ for Melo's method. As stated in remark 6, the sole FFT gives a large approximation error in the high-frequency part. However, an accurate model is restored after using the IFFT and transfer function modeling.

Example 2. Consider the Doukas and Luyben plant:[4]

$$\mathbf{G}(s) = \begin{bmatrix} \frac{-9.811e^{-1.59}s}{11.36s+1} & \frac{0.374e^{-7.75s}}{22.22s+1} & \frac{-2.368e^{-27.33s}}{33.3s+1} & \frac{-11.3e^{-3.79s}}{(21.74s+1)^2} \\ \frac{5.984e^{-2.24s}}{14.29s+1} & \frac{-1.986e^{-0.71s}}{66.67s+1} & \frac{0.422e^{-8.72s}}{(250s+1)^2} & \frac{5.24e^{-60s}}{400s+1} \\ \frac{2.38e^{-0.42s}}{(1.43s+1)^2} & \frac{0.0204e^{-0.59s}}{(7.14s+1)^2} & \frac{0.513e^{-s}}{s+1} & \frac{-0.33e^{-0.68s}}{(2.38s+1)^2} \\ \frac{-11.3e^{-3.79s}}{(21.74s+1)^2} & \frac{-0.176e^{-0.48s}}{(6.9s+1)^2} & \frac{15.54e^{-s}}{s+1} & \frac{4.48e^{-0.52s}}{11.11s+1} \end{bmatrix}$$

under the control of the decentralized PI controller:[4]

$$\mathbf{K}(s) = \begin{bmatrix} -0.084\left(1+\frac{s}{33}\right) & 0 & 0 & 0 \\ 0 & -5.16\left(1+\frac{s}{15.5}\right) & 0 & 0 \\ 0 & 0 & 0.305\left(1+\frac{s}{17.0}\right) & 0 \\ 0 & 0 & 0 & 0.529\left(1+\frac{s}{11.2}\right) \end{bmatrix}$$

A closed-loop sequential step experiment is performed. The proposed method yields Chart 1 with the errors

$$\epsilon = [0.5251\% \;\; 1.5227\% \;\; 0.0638\% \;\; 0.5674\%]^{\mathrm{T}}$$

and

$$E = \begin{bmatrix} 0.5085\% & 0.2513\% & 0.0635\% & 0.7372\% \\ 1.125\% & 0.1598\% & 5.3791\% & 0.4579\% \\ 0.6353\% & 0.1221\% & 0.5281\% & 0.3321\% \\ 0.7047\% & 0.3921\% & 0.5328\% & 0.2944\% \end{bmatrix}$$

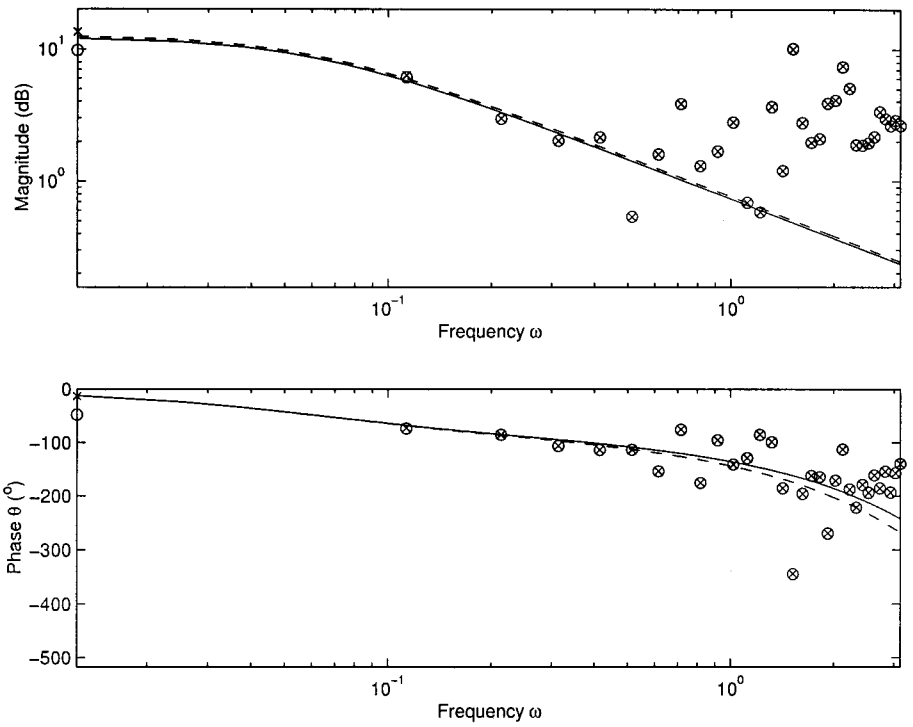

Figure 3. Bode plots for G_{11} of the WB plant under NSR = 30%: - - -, actual plant; —, estimated model; ×, proposed FFT; ○, Melo's method.

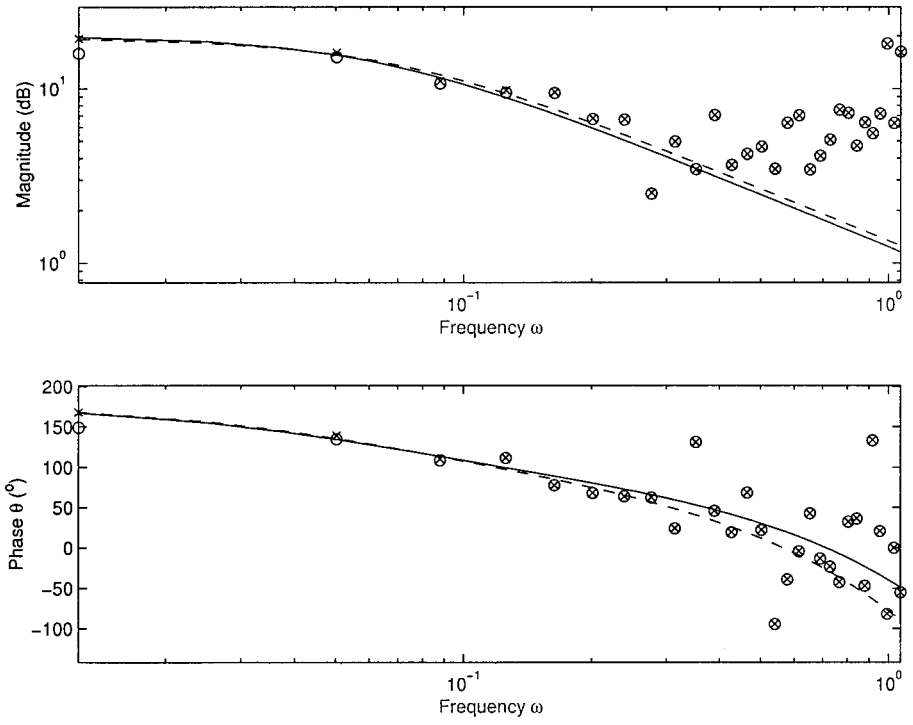

Figure 4. Bode plots for G_{22} of the WB plant under NSR = 30%: - - -, actual plant; —, estimated model; ×, proposed FFT; ○, Melo's method.

Chart 1

$$\hat{G}(s) = \begin{bmatrix} \frac{-9.8111e^{-1.5867s}}{11.4106s+1} & \frac{0.3740e^{-7.7555s}}{22.2658s+1} & \frac{-2.3678e^{-27.3198s}}{33.3231s+1} & \frac{-11.2999e^{-3.7318s}}{475.0586s^2+43.5833s+1} \\ \frac{5.9975e^{-2.2277s}}{14.4527s+1} & \frac{-1.9849e^{-0.7108s}}{66.6687s+1} & \frac{0.3993e^{-8.6505s}}{59221s^2+471s+1} & \frac{5.2268e^{-60.4408s}}{397.4322s+1} \\ \frac{2.3800e^{-0.4164s}}{2.0578s^2+2.8695s+1} & \frac{0.0204e^{-0.5882s}}{51.0132s^2+14.2885s+1} & \frac{0.5130e^{-1.0012s}}{1.0045s+1} & \frac{-0.3300e^{-0.6853s}}{5.6436s^2+4.7611s+1} \\ \frac{-11.3000e^{-3.7347s}}{474.9052s^2+43.5817s+1} & \frac{(-0.0051s-0.1760)e^{-0.5032s}}{47.7076s^2+13.8112s+1} & \frac{15.5400e^{-1.0010s}}{1.0049s+1} & \frac{4.4800e^{-0.5211s}}{11.1146s+1} \end{bmatrix}$$

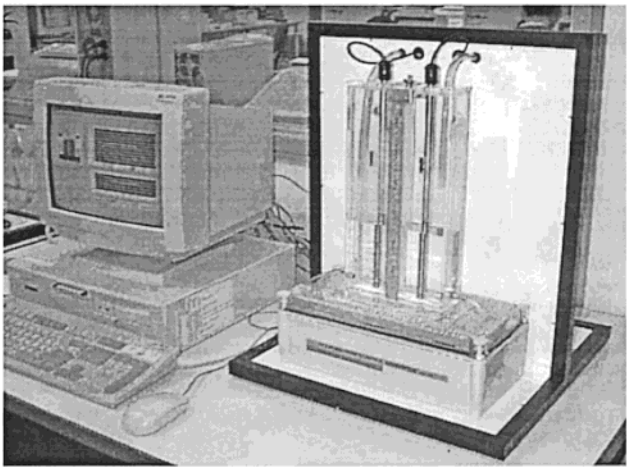

Figure 5. Coupled-tank level control system.

respectively. The effectiveness of the proposed method is clearly noticed.

4. Real-Time Experiment

In this section, the proposed identification method is applied to a coupled-tank control apparatus, made by KentRidge Instrument Ptd. Ltd, Singapore. The process consists of two small tower-type tanks mounted above a reservoir which functions as a storage for the water (Figure 5). Each tank level is controlled by manipulating the voltage to the pump.

A closed-loop sequential step experiment was carried out on the process, and the proposed method is used to give the model

$$\hat{G}(s) = \begin{bmatrix} \dfrac{2.7138}{33.4664s+1}e^{-5.4281s} & \dfrac{2.5042}{33.2692s+1}e^{-11.4657s} \\ \dfrac{2.3222}{31.7212s+1}e^{-11.5917s} & \dfrac{2.7306}{31.0345s+1}e^{-10.1784s} \end{bmatrix}$$

with the error

$$\epsilon = \begin{bmatrix} 0.16\% \\ 0.14\% \end{bmatrix}$$

The responses are shown in Figure 6, where y is from the actual process and $\hat{y}$ is from the simulation with the estimated model under the same recorded u. The effectiveness of the proposed method is clear.

5. Conclusions

In this paper, a novel method has been developed for robust identification of linear time-invariant multivariable processes. The FFT and IFFT techniques are used to construct the process step response from the test data, from which the FOPDT/SOPDT model is estimated for each element. The method can accommodate a wide range of experiments, including step or relay, open-loop or closed-loop, provided that the test signals are persistently exciting and the experiment produces steady-state responses. The proposed method is shown to be accurate and robust.

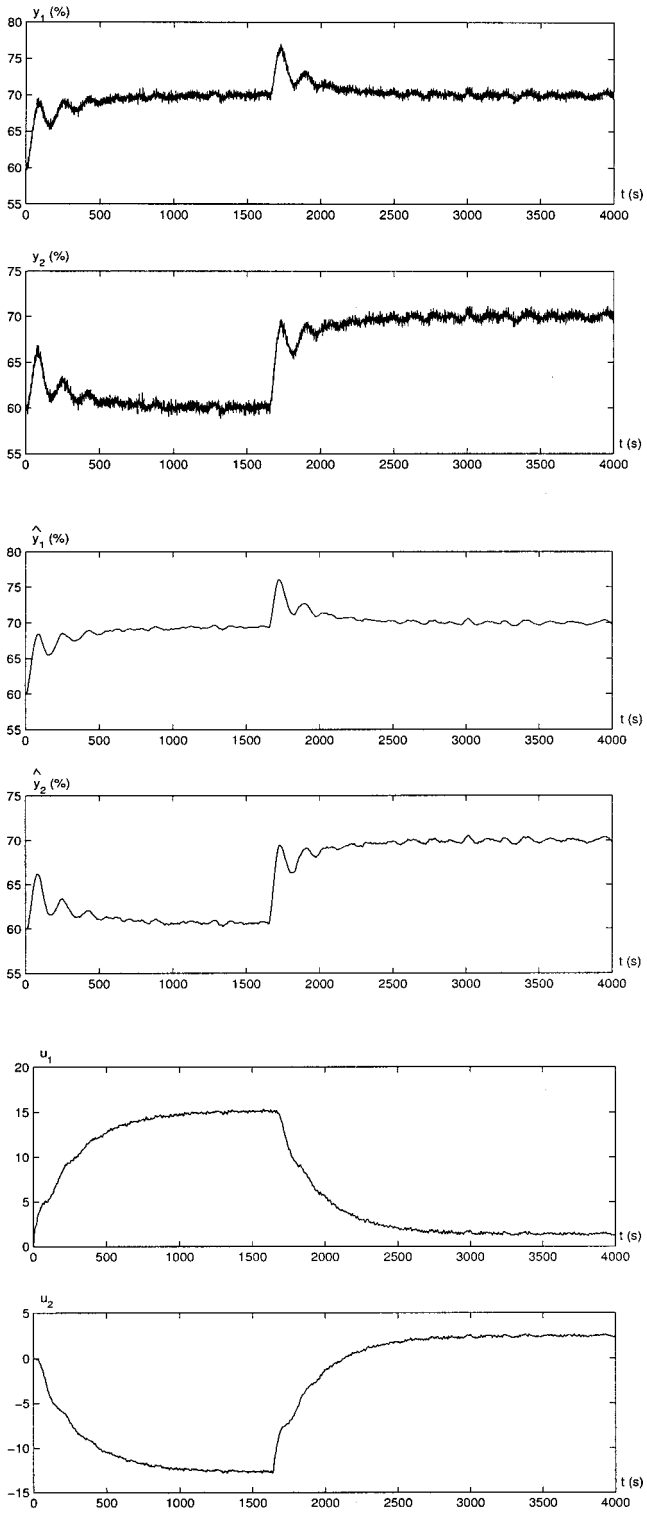

Figure 6. Responses of the coupled-tank system.

Literature Cited

(1) Wang, Q. G.; Hang, C. C.; Zou, B. Frequency Response Approach to Autotuning of Multivariable Controllers. *Chem. Eng. Res. Des.* **1997**, *75*, 797.

(2) Schoukens, J.; Rolain, Y.; Pintelon, R. Improved Frequency Response Function Measurements for Random Noise Excitations. *IEEE Trans. Instrum. Meas.* **1998**, *47*, 322.

(3) Garcia, C. E.; Morari, M. Internal Model Control: A Unifying Review and Some New Results. *Ind. Eng. Chem. Process Des. Dev.* **1982**, *21*, 308.

(4) Luyben, W. L. Simple Method for Tuning SISO Controllers in Multivariable System. *Ind. Eng. Chem. Process Des. Dev.* **1986**, *25*, 654.

(5) Rao, M.; Xia, Q. J.; Ying, Y. Q. *Modeling and Advanced Control for Process Industries*; Springer-Verlag: London, 1994.

(6) Shiu, S. J.; Hwang, S. H. Sequential Design Method for Multivariable Decoupling and Multiloop PID Controllers. *Ind. Eng. Chem. Res.* **1998**, *37*, 107.

(7) Pintelon, R.; Guillaume, P.; Rolain, Y.; Schoukens, J.; Hamme, H. V. Parametric Identification of Transfer Functions in the Frequency Domain—A Survey. *IEEE Trans. Autom. Control* **1994**, *39*, 2245.

(8) Forssell, U.; Ljung, L. Closed-loop Identification Revisited. *Automatica* **1999**, *35*, 1215.

(9) Unbehauen, H.; Rao, G. P. *Identification of Continuous Systems*; Elsevier Science: Amsterdam, The Netherlands, 1987.

(10) Rake, H. Step Response and Frequency Response Methods. *Automatica* **1980**, *16*, 519.

(11) Astrom, K. J.; Hagglund, T. *PID Controllers: Theory, Design, and Tuning*, 2nd ed.; ISA: Research Triangle Park, NC, 1995.

(12) Bi, Q.; Cai, W. J.; Lee, E. L.; Wang, Q. G.; Hang, C. C.; Zhang, Y. Robust Identification of First-order Plus Dead-time Model from Step Response. *Control Eng. Pract.* **1999**, *7*, 71.

(13) Yuwana, M.; Seborg, D. E. A New Method for On-line Controller Tuning. *AIChE J.* **1982**, *28*, 434.

(14) Jutan, A.; Rodriguez, E. S., II. Extension of a New Method for On-line Controller Tuning. *Can. J. Chem. Eng.* **1984**, *62*, 802.

(15) Lee, J. On-line PID Controller Tuning from a Single, Closed-loop Test. *AIChE J.* **1989**, *35*, 329.

(16) Suganda, P.; Krishnaswamy, P. R.; Rangaiah, G. P. On-line Process Identification from Closed-loop Tests Under PI Control. *Trans. Inst. Chem. Eng.* **1998**, *76*, 451.

(17) Melo, D. L.; Friedly, J. C. On-line, Closed-loop Identification of Multivariable Systems. *Ind. Eng. Chem. Res.* **1992**, *31*, 274.

(18) Astrom, K. J.; Hagglund, T. Automatic Tuning of Simple Regulators with Specification on Phase and Amplitude Margins. *Automatica* **1984**, *20*, 645.

(19) Loh, A. P.; Hang, C. C.; Quek, C. K.; Vasnani, V. U. Autotuning of Multiloop Proportional-integral Controllers Using Relay Feedback. *Ind. Eng. Chem. Res.* **1993**, *32*, 1102.

(20) Schoukens, J.; Pintelon, R.; Van Der Ouderaa, E.; Rennboog, J. Survey of Excitation Signals for FFT Based Signal Analyzers. *IEEE Trans. Instrum. Meas.* **1988**, *37*, 342.

(21) Pintelon, R.; Biesen, L. V. Identification of Transfer Functions with Time Delay and Its Application to Cable Fault Location. *IEEE Trans. Instrum. Meas.* **1990**, *39*, 479.

(22) Soderstrom, T.; Stoica, P. *System identification*; Prentice-Hall: Englewood Cliffs, NJ, 1989.

(23) Wang, Q. G.; Lee., T. H.; Bi, Q. Use of FFT in Relay Feedback Systems. *Electron. Lett.* **1997**, *33*, 1099.

(24) Cartwright, M. *Fourier Methods for Mathematicians, Scientists and Engineers*; Ellis Horwood: New York, 1990.

(25) Morrison, N. *Introduction to Fourier Analysis*; John Wiley & Sons Inc.: New York, 1994.

(26) Kuhfitting, P. K. F. *Introduction to the Laplace Transform*; Plenum Press: New York, 1978.

(27) Wang, Q. G.; Hang, C. C.; Bi, Q. A Technique for Frequency Response Identification from Relay Feedback. *IEEE Trans. Control Syst. Technol.* **1999**, *7*, 122.

(28) Prett, D. M.; Morari, M. *The Shell Process Control Workshop*; Butterworth Publishers: Houston, TX, 1987.

(29) Luyben, M. L.; Luyben, W. L. *Essentials of Process Control*; Butterworth Publishers: New York, 1997.

(30) Wang, Q. G.; Zhang, Y. Novel robust multivariable process identification. National University of Singapore. Personal communication, 1999.

(31) Wang, Q. G.; Zhang, Y. Robust identification of continuous time delay systems from step responses. *Automatica* **1999**, submitted for publication.

(32) Zhu, Y. C.; Backx, T. *Identification of Multivariable Industrial Process: for Simulation, Diagnosis and Control*; Springer-Verlag: London, 1993.

(33) Haykin, S. *An Introduction to Analogue & Digital Communications*; John Wiley & Sons: New York, 1989.

(34) Wood, R. K.; Berry, M. W. Terminal Composition Control of a Binary Distillation Column. *Chem. Eng. Sci.* **1973**, *28*, 1707.

Received for review November 12, 1999
Revised manuscript received January 26, 2001
Accepted March 14, 2001

IE9908175